Vapor-Liquid-Liquid Equilibrium of the *n*-Pentane–Sulfur Dioxide–Benzene System at 0° F.

WARREN W. BOWDEN[1], JOHN C. STATON[2], and BUFORD D. SMITH[3]
School of Chemical Engineering, Purdue University, West Lafayette, Ind.

Vapor-liquid-liquid equilibrium data are reported for the *n*-pentane–sulfur dioxide–benzene system and its associated binaries at 0° F. A set of data on the benzene-pentane binary at 60° F. is also reported. Twenty-five data points are reported on the *n*-pentane–sulfur dioxide–benzene–*n*-hexane quaternary system at 0° F. A new type of static cell was used. The liquid and vapor samples were analyzed by gas chromatography. The data were checked for consistency by use of integrated forms of the Gibbs-Duhem equation and by fitting with the Redlich-Kister equation using a least squares procedure.

A STATIC cell was developed which made it possible to study the phase equilibrium behavior of the three-phase ternary, *n*-pentane–sulfur dioxide–benzene, at 0° F. Equilibrium data at 0° F. also were obtained on the *n*-pentane–sulfur dioxide and *n*-pentane–benzene binaries. The *n*-pentane–benzene system was also studied at 60.8° F. A small amount of data on the *n*-pentane–sulfur dioxide–benzene–*n*-hexane quaternary at 0° F. are also reported. Analyses of the liquid and gas phases were made by gas chromatography. The data were smoothed using an integrated form of the Gibbs-Duhem equation and correlated using the Redlich-Kister expressions.

EXPERIMENTAL

Analytical Methods. A Perkin-Elmer 154-C chromatography unit was used for all sample analyses. The methods used for calibration and calculation of sample compositions have been described (*16, 17*). It was estimated that accuracy was 5% or better on most samples. Further details are available (*2*).

Apparatus. Figure 1 gives a general idea of the construction of the cell. The cell body, pistons, and cylinders were machined from stainless steel. All threaded connections were made tight by Viton rubber O-rings. While the cell was being charged through line 26, liquid levels could be observed through windows 18 using a periscope tube (not shown in Figure 1). Agitation was provided by paddle 19 which rotated at approximately 30 r.p.m.

Data (*2*) indicated that equilibrium was virtually attained in approximately 30 minutes. In actual practice a minimum of 4 hours was allowed for complete equilibrium. After equilibrium had been reached, liquid samples were captured by the small pistons, 4, and displaced into sample vials through line 11 by mercury. The pistons were actuated by dry nitrogen through lines 9 and 15. Initially the gas sample was captured by the large piston and displaced by mercury into a gas holder before being analyzed in the chromatography unit. However, because of adsorption effects (*1, 2*), this procedure was abandoned and the gas sample was taken off the top of the cell through line 27 directly to the chromatography unit. Because of the large gas (1000 to 1900 cc.) and liquid (800 to 1700 cc.) phase volumes, removal of the small (ca. 10 cc.) gas sample did not measurably disturb the equilibrium of the system in the cell.

The entire cell was submerged in a 50 weight % water-ethylene glycol solution in a Wilkens-Anderson cold bath and maintained at 0° F. by a precision microset thermoregulator, No. 62542, manufactured by the Precision Scientific Co. It was estimated that the temperature was maintained within 0.05° F. of 0° F., on the average.

Materials. The pure component reagents used in this study were: sulfur dioxide, anhydrous grade (99.98%, minimum) from the Matheson Co.; *n*-pentane and *n*-hexane, pure grade (99 mole %, minimum) obtained from the Phillips Petroleum Co.; spectrograde benzene from Matheson, Coleman, and Bell. The above materials were checked for impurities by gas chromatography. No impurities were detected in the sulfur dioxide; impurities to the extent of about 0.2 weight % were detected in the *n*-pentane and *n*-hexane, and about 0.1 weight % in the benzene. These materials were used without further purification.

Procedure. Vapor and liquid compositions and total pressures were measured using the equipment and techniques described above. These measurements were used in Equation 1

$$\ln \gamma_i = \ln \frac{y_i p}{x_i p_i^*} + \left(\frac{B_i - V_i^L}{RT}\right)(p - p_i^*) \qquad (1)$$

to calculate activity coefficients of the various components. The assumptions underlying Equation 1 are that the gas-phase solution is ideal; the gas-phase PVT behavior can be adequately represented by the virial equation of state, using terms up to and including the second; and the liquid volume, V_i^L, is independent of pressure. The second virial coefficients, B_i, were estimated using the generalized correlation of Pitzer and Curl (*6*). The liquid molar volumes, V_i^L, and vapor pressures, p_i^*, were taken from the literature (*4, 8, 9*). Total pressures developed by the systems studied were of the order of 300 mm. of Hg and hence the second term in Equation 1 was small in comparison with the first. For this reason any inaccuracies in the estimated virial coefficients had a rather small effect on the values of the activity coefficients.

Benzene activity coefficients in mixtures containing solid benzene were calculated in a different way. For a system in equilibrium, if the same standard state is used for both phases,

[1] Present address, Rose Polytechnic Institute, Terre Haute, Ind.
[2] Present address, Humble Oil and Refining Co, Baytown, Tex.
[3] Present address, Washington University, St. Louis, Mo.

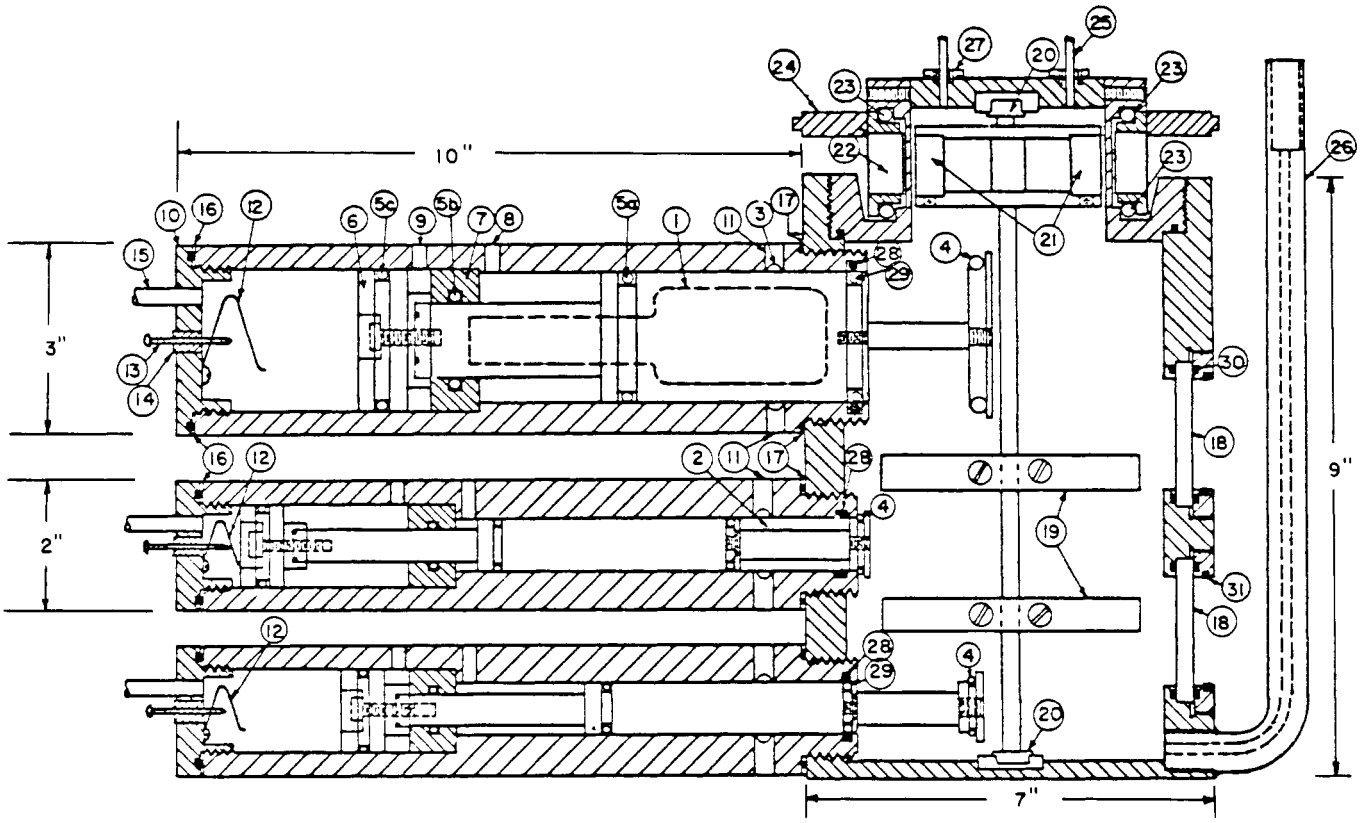

Figure 1. Cross section of cell

1. Hollowed-out gas sample piston
2. Liquid sample chamber
3. Groove in sample chamber
4. Teflon O-rings
5a, 5b, 5c. Viton rubber O-rings
6. Driving piston
7. Insert ring
8. Vacuum tap
9. Nitrogen tubing connection
10. Cylinder end cap
11. Sample tubing connection
12. Spring contacts for lights indicating position of pistons
13. Brass machine screw
14. Teflon insulator
15. Nitrogen tubing connection
16. Viton O-rings
17. Viton O-rings
18. Window
19. Agitator
20. Stirrer shaft bearings
21. Inner magnets
22. Outer magnets
23. Ball bearings
24. Outer magnet carrier ring
25. Tubing connecting cell to absolute manometer
26. Feed line
27. Gas sample line
28. Teflon O-ring
29. Teflon O-ring in piston
30. Ring and Viton O-ring making seal around window
31. O-ring making seal between cell and periscope tube

$$\bar{a}_B = a^s_B \tag{2}$$

$$\gamma_B = \frac{\bar{a}_B}{x_B} = \frac{\bar{f}_B}{f^o_B x_B} = \frac{a^s_B}{x_B} = \frac{f^s_{B,p}}{f^L_{B,p} x_B} \tag{3}$$

The $f^s_{B,p}$ and $f^L_{B,p}$ can be calculated from

$$\ln f_{B,p} = \ln p^*_B + \frac{1}{RT}\left[V_B p + p^*_B (B_B - V_B)\right] \tag{4}$$

The assumptions implicit in Equation 4 are that the gas-phase PVT nonideality is adequately represented by the second virial coefficient and that the solid or liquid volume is independent of pressure. Combination of Equations 3 and 4 gives

$$\gamma_B = \frac{0.7236}{x_B} \tag{5}$$

The major experimental difficulties encountered in this work resulted from the low system temperature (0° F.), the subatmospheric system pressure, and the fact that the maximum concentration of benzene in the vapor phase was around 10% in the pentane-benzene system and about 3% in the sulfur dioxide–benzene system.

RESULTS

Binary Equilibrium Data. Complete experimental data on the *n*-pentane (1)–benzene (3) system at 0° and 60.8° F. are given in Table I. The 0° F. data are also presented in graphical form in Figures 2 and 3 as curves of γ_i *vs.* x_3. Solid benzene is present in the region at the right of the vertical dashed line at $x_3 = 0.54$. The value of γ_3 calculated from Equation 5 is indicated as an open circle.

These data were checked for consistency by integration of the Gibbs-Duhem equation in the manner suggested by Dodge (*3*). Assumed values of γ_3 were used to calculate values of γ_1. The solid curves in Figure 2 give the results of these calculations. The agreement of the consistent curves with the experimental points leads to the conclusion that the data are generally consistent.

Direct quantitative comparison of the above data with the isobaric data of Myers (*5*) is not possible. However, the two sets of data appear to be in substantial agreement.

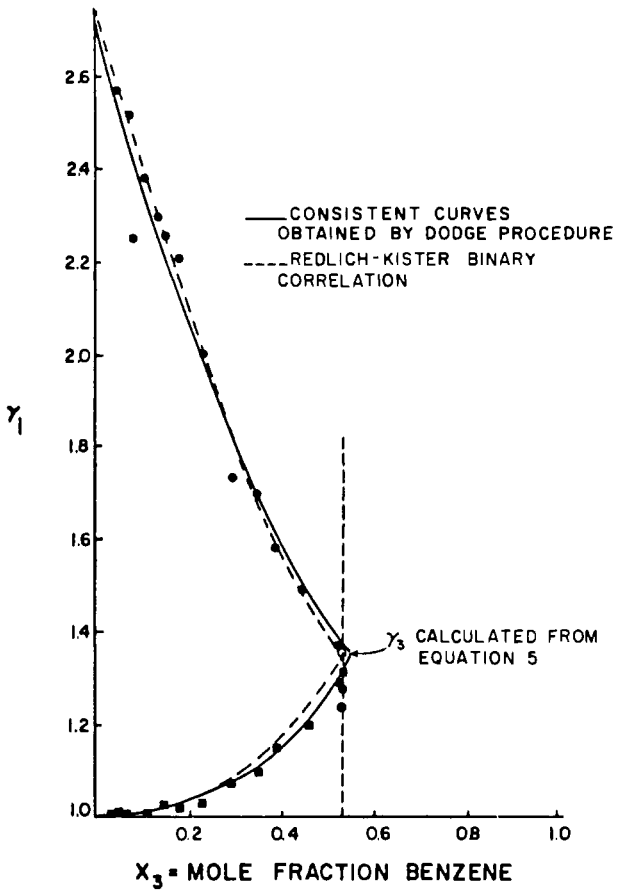

Figure 2. Activity coefficients for *n*-pentane (■)–benzene (●) system at 0° F. (run 8)

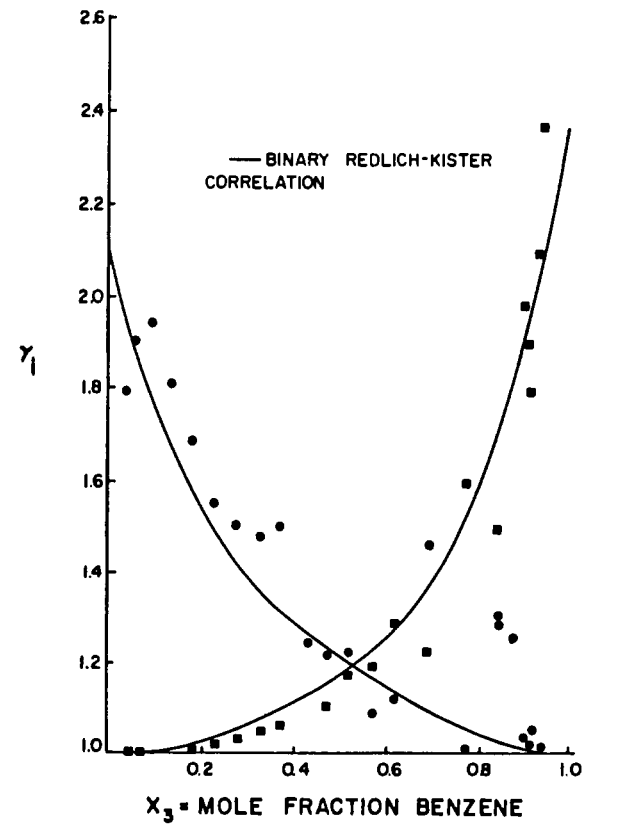

Figure 3. Activity coefficients for *n*-pentane (●)–benzene (■) system at 60.8° F. (run 7)

Table I. Binary Phase and Activity Coefficient Data for the *n*-Pentane (1)–Benzene (3) System

Sample	$P_{mm.\ Hg}$	x_1	y_1	γ_1	x_3	y_3	γ_3
			Run 7 at 60.8° F.				
1	117.3	0.081	0.439	1.792	0.919	0.561	1.151
2	153.5	0.159	0.553	1.502	0.841	0.447	1.306
3	127.0	0.098	0.542	1.980	0.902	0.458	1.036
4	108.0	0.066	0.453	2.099	0.934	0.547	1.017
5	98.5	0.052	0.448	2.376	0.948	0.552	0.924
6	117.5	0.089	0.513	1.900	0.911	0.487	1.011
7	138.0	0.124	0.503	1.569	0.876	0.497	1.258
8	150.5	0.156	0.551	1.494	0.844	0.449	1.283
9	177.5	0.225	0.722	1.594	0.775	0.278	1.018
10	196.5	0.301	0.675	1.229	0.699	0.325	1.461
11	217.0	0.374	0.797	1.290	0.626	0.203	1.122
12	221.0	0.423	0.822	1.196	0.577	0.178	1.089
13	241.5	0.479	0.833	1.171	0.521	0.167	1.227
14	245.5	0.525	0.852	1.109	0.475	0.148	1.215
15	262.5	0.561	0.869	1.130	0.439	0.131	1.243
16	275.0	0.625	0.871	1.064	0.375	0.129	1.506
17	283.0	0.665	0.889	1.050	0.335	0.111	1.481
18	293.5	0.715	0.908	1.033	0.285	0.092	1.507
19	305.5	0.761	0.923	1.027	0.239	0.077	1.553
20	316.5	0.815	0.937	1.008	0.185	0.063	1.689
21	326.3	0.857	0.949	1.000	0.143	0.051	1.812
22	338.0	0.896	0.962	1.003	0.104	0.038	1.941
23	346.0	0.934	0.977	0.999	0.066	0.023	1.904
24	351.5	0.956	0.986	1.001	0.044	0.014	1.791
			Run 8 at 0° F.				
1	53.0	0.461	0.896	1.352	0.539	0.104	1.231
4	51.5	0.463	0.889	1.301	0.537	0.111	1.278
5	52.5	0.475	0.886	1.287	0.525	0.114	1.363
6	55.5	0.546	0.898	1.200	0.454	0.102	1.488
7	58.0	0.607	0.911	1.143	0.393	0.089	1.580
8	59.0	0.650	0.916	1.093	0.350	0.084	1.690
9	61.5	0.700	0.930	1.072	0.300	0.070	1.728
10	64.0	0.768	0.940	1.027	0.232	0.060	1.993
11	67.0	0.818	0.949	1.021	0.182	0.050	2.200
12	69.0	0.847	0.958	1.025	0.153	0.042	2.252
13	69.5	0.867	0.963	1.013	0.133	0.037	2.290
14	70.7	0.895	0.970	1.006	0.105	0.030	2.378
15	72.5	0.919	0.979	1.013	0.081	0.021	2.245
16	73.0	0.935	0.981	1.004	0.065	0.019	2.514
17	74.0	0.949	0.984	1.006	0.051	0.016	2.805
18	74.5	0.960	0.989	1.005	0.040	0.011	2.561

The dashed curves in Figure 2 are those obtained by a least squares fit of the data to the three-constant Redlich-Kister (7) form given in Equation 6.

$$\log \gamma_i = x_j^2 \{ B_{ij} + C_{ij}[(x_i - x_j) + 2x_i] + D_{ij}[(x_i - x_j)^2 + 4x_i(x_i - x_j)] \} \quad (6)$$

The least squares procedure involved use of a residual function defined by Equation 7:

$$R_{i,k} = \{ f_i[B_{ij}, C_{ij}, D_{ij}, x_i(k)] - \log \gamma_{i,\,exp.} \}$$
$$i = 1,2$$
$$k = 1,2, \ldots ,n \quad (7)$$

where f_i is the function defined by Equation 6. The function minimized was the sum, S_m, defined by Equation 8.

$$S_m = \sum_k (R_{i,k}^2 + R_{j,k}^2 + \ldots) \quad (8)$$

This procedure is preferable to the use of a residual involving $\log \gamma_i/\gamma_j$ in that it can be applied to multicomponent systems and that experimental activity coefficients of individual components can be weighted. The correlation represented by Equation 6 gave an S_m of 0.137 for the 16 points in the 0° F. data.

The data on the *n*-pentane–benzene system at 60.8° F. are presented graphically in Figure 3. The smooth curves were obtained by a least squares fit of the data with a three-constant Redlich-Kister expression. These data were taken

Table II. Binary Phase and Activity Coefficient Data for the Sulfur Dioxide(2)–Benzene (3) System

Sample	$P_{mm. Hg}$	x_2	y_2	γ_2	x_3	y_3	γ_3
			Run 10				
1	517.0	0.965	0.999	1.009	0.0345	0.001	1.992
2	501.5	0.938	0.998	1.006	0.062	0.002	1.726
3	481.5	0.905	0.997	1.002	0.095	0.003	1.678
4	472.0	0.870	0.996	1.021	0.130	0.004	1.596
5	458.5	0.840	0.995	1.026	0.160	0.005	1.504
6	443.0	0.802	0.994	1.038	0.197	0.006	1.408
7	429.5	0.770	0.994	1.048	0.230	0.006	1.335
8	414.5	0.728	0.993	1.070	0.272	0.007	1.276
9	394.0	0.682	0.991	1.085	0.318	0.009	1.206
10	382.5	0.660	0.990	1.088	0.340	0.010	1.211
11	361.2	0.619	0.988	1.095	0.381	0.011	1.230
12	355.0	0.588	0.988	1.132	0.412	0.012	1.205
13	335.5	0.558	0.986	1.127	0.442	0.013	1.171
14	318.5	0.520	0.984	1.146	0.480	0.016	1.218
15	307.5	0.498	0.982	1.154	0.502	0.018	1.251
16	260.0	0.436	0.979	1.112	0.564	0.021	1.123
17	249.5	0.414	0.977	1.120	0.585	0.023	1.146
18	234.2	0.377	0.974	1.152	0.623	0.026	1.145
19	205.0	0.340	0.969	1.115	0.660	0.031	1.131

Table III. Redlich-Kister Constants for Binary Systems

Systems	B_{ij}	C_{ij}	D_{ij}
Pentane (1)–sulfur dioxide (2)[a]	1.1841	−0.2500	...
Pentane (1)–benzene (3)	0.5008	−0.0561	−0.0042
Sulfur dioxide (2)–benzene (3)	0.2430	−0.0477	0.1598

[a] Calculated from solubility data according to method described by Smith (*14*).

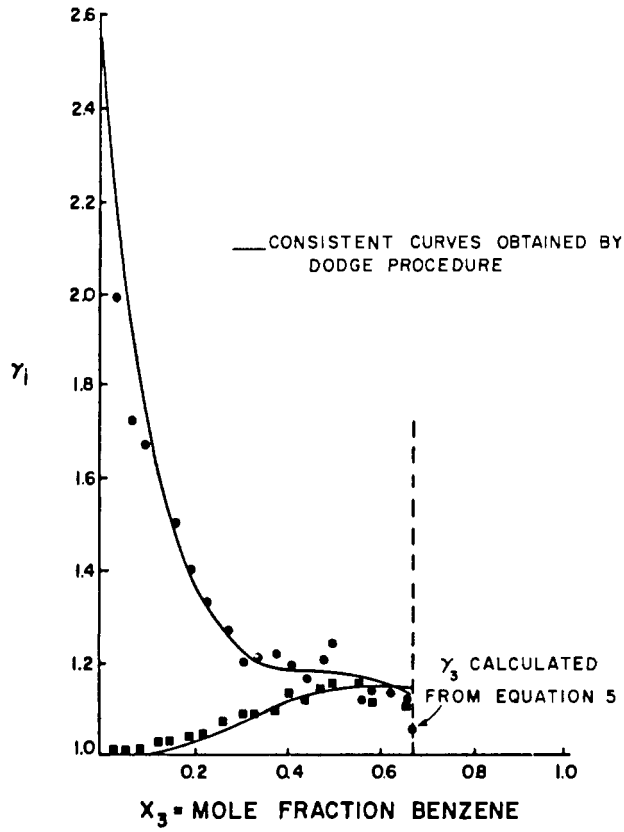

Figure 4. Activity coefficients for sulfur dioxide (■)–benzene (●) system at 0° F. (run 10)

during an early period in the research when sampling techniques were still being developed. Even though the quality of the 60.8° F. data is not equal to that of later work, it is included because of possible future use in the determination of the effect of temperature on correlation constants.

Complete experimental data on the sulfur dioxide(2)–benzene(3) system at 0° F. are given in Table II, and shown graphically in Figure 4, where the smooth curves were obtained by the Dodge procedure. Solid benzene is present in the region at the right of the vertical dashed line at $x_3 = 0.63$. The value of γ_3 calculated from Equation 5 is indicated by an open circle. Inspection of Figure 4 leads to to the conclusion that these data, on the whole, are consistent.

The Redlich-Kister binary constants obtained in this work are tabulated in Table III.

Further correlation of the above binary data (*2*) showed that the least squares procedure described above gave approximately the same results as the procedure involving correlation of log γ_i/γ_j and that three constants were adequate to describe the data.

Ternary Equilibrium Data. Complete experimental data on the ternary system *n*-pentane (1)–sulfur dioxide (2)–benzene (3) are given in Table IV, where sample numbers followed by an R indicate a pentane-rich phase and those followed by an S indicate a sulfur dioxide–rich phase. This notation is used only for samples of three-phase systems. Table V gives benzene activity cofficients in systems containing solid benzene which were calculated from experimental data by Equation 5. Column 6 in Table V gives values predicted by Ternary Correlation II (described below) for comparison. The solubility envelope and tie-line data agree generally with those of Satterfield *et al.* (*10*) on sulfur dioxide–paraffinic-aromatic systems. Liquid-liquid-vapor equilibrium data of the type presented in this paper have been reported previously only for very few systems. Smirnova, Morachevsky, and Storonkin (*12*) reported data on the propanol-*n*-propyl acetate–water system, and Udovenko and Fatkulina (*18*) reported data on the ethanol-dichloroethane-water system.

The consistency of the ternary data was checked and smoothed values of γ_1, γ_2, and γ_3 were obtained by application of integrated forms of the Gibbs-Duhem equation to several paths across Figures 5, 6, and 7. The integrated forms and procedure are described by Smith (*13*). Schuhmann's graphical method (*11*) was also used.

The smoothed activity coefficients, obtained as described above, are presented in Figures 5, 6, 7, and 9. (Tabulated values are presented in an ADI document.) The relatively high values of γ_1 and γ_2 are to be noted in Figures 5 and 6. Figures 5 and 6 (dashed curves) also present values of γ_1 and γ_2 predicted by a Redlich-Kister correlation described below. Curves of γ_3 predicted by this correlation are presented in Figure 9 (deposited with ADI). Figure 7 gives the unexpected result that in the vicinity of $x_1 = 0.25$, $x_3 = 0.25$, values of γ_3 are close to unity. All of the binaries in this system exhibit positive deviations and for this reason it is believed that the benzene activity coefficients should be equal to or greater than 1 throughout the diagram.

Isobars of total pressure calculated from the smoothed activity coefficients using Equation 1 are presented in Figure 8.

The above smoothed data were compared with the experimental data shown in Table IV. Smoothed values at the experimental compositions were obtained by interpolating the tabulated smoothed values given by Bowden (*2*). For the 83 ternary points, the sums of squares of deviations of the smoothed activity coefficients from the experimental values for components one, two, and three, were 14.4, 2.2, and 37.6, respectively. Elimination of four experimental points from the comparison reduced these sums by approximately 80, 50, and 90%, respectively.

The ternary data were correlated by Redlich-Kister forms

Table IV. Phase and Activity Coefficient Data

Sample	$P_{mm.\ Hg}$	x_1	x_2	y_1	y_2	γ_1	γ_2	γ_3
				Run 9				
1	249.7	0.922	0.047	0.317	0.679	1.102	6.902	3.238
2	394.5	0.871	0.100	0.192	0.806	1.097	6.013	2.506
3	444.7	0.851	0.121	0.174	0.825	1.137	5.724	2.566
4	473.5	0.832	0.140	0.152	0.846	1.083	5.399	2.223
5	501.5	0.814	0.158	0.150	0.848	1.152	5.063	2.616
6R	585.6	0.776	0.217	0.128	0.871	1.193	4.419	5.833
7R	578.0	0.764	0.221	0.135	0.865	1.256	4.257	2.872
8R	575.0	0.742	0.235	0.121	0.878	1.161	4.041	1.631
9R	575.1	0.720	0.250	0.133	0.866	1.311	3.747	1.718
10R	564.5	0.698	0.262	0.123	0.876	1.227	3.545	1.280
11R	558.0	0.678	0.273	0.124	0.875	1.258	3.369	1.102
12R	555.0	0.640	0.300	0.128	0.871	1.369	3.032	1.472
13R	549.5	0.617	0.316	0.127	0.872	1.402	2.849	1.167
14R	554.0	0.611	0.323	0.122	0.876	1.366	2.832	1.453
15R	546.5	0.594	0.330	0.118	0.881	1.341	2.743	1.269
16R	542.0	0.561	0.356	0.125	0.874	1.493	2.505	1.062
17R	538.5	0.526	0.382	0.120	0.878	1.524	2.333	1.388
18R	535.5	0.471	0.427	0.121	0.877	1.712	2.070	1.036
19R	531.0	0.404	0.489	0.121	0.877	1.969	1.798	1.300
6S	585.0	0.051	0.942	0.128	0.871	18.02	1.018	6.221
7S	578.0	0.066	0.917	0.135	0.865	14.52	1.025	2.649
8S	575.0	0.066	0.909	0.121	0.878	12.98	1.045	1.493
9S	575.1	0.070	0.899	0.133	0.866	13.43	1.042	1.713
10S	564.5	0.076	0.833	0.123	0.876	11.27	1.054	1.228
11S	558.0	0.085	0.865	0.124	0.875	10.05	1.063	1.069
12S	555.0	0.091	0.850	0.128	0.871	9.625	1.070	1.497
13S	549.5	0.106	0.825	0.127	0.872	8.180	1.093	1.125
14S	554.0	0.104	0.825	0.122	0.876	8.062	1.108	1.336
15S	546.5	0.107	0.814	0.118	0.881	7.438	1.113	1.223
16S	542.0	0.120	0.793	0.125	0.874	6.978	1.124	1.016
17S	538.5	0.132	0.773	0.120	0.878	6.073	1.151	1.359
18S	535.5	0.175	0.722	0.121	0.877	4.591	1.225	1.030
19S	531.0	0.396	0.495	0.121	0.877	2.009	1.773	1.288
20	525.0	0.411	0.475	0.125	0.873	1.974	1.820	1.208
21	520.5	0.414	0.464	0.124	0.874	1.926	1.850	1.121
22	513.0	0.420	0.444	0.123	0.874	1.875	1.903	1.065
23	508.0	0.413	0.446	0.124	0.874	1.892	1.878	1.050
24	501.0	0.431	0.416	0.128	0.868	1.854	1.972	1.202
25	488.0	0.427	0.409	0.125	0.872	1.776	1.966	1.016
26	481.5	0.449	0.380	0.130	0.866	1.735	2.073	1.217
27	465.0	0.451	0.366	0.131	0.864	1.694	2.074	1.205
28	452.9	0.456	0.349	0.132	0.863	1.647	2.120	1.131
29	440.0	0.457	0.336	0.136	0.859	1.643	2.128	1.197
30	419.2	0.461	0.303	0.139	0.855	1.591	2.237	1.181
31	406.0	0.452	0.301	0.144	0.850	1.623	2.172	1.186
32	388.0	0.447	0.288	0.145	0.848	1.590	2.165	1.144
33	376.0	0.454	0.271	0.160	0.832	1.675	2.189	1.173
34	355.8	0.453	0.252	0.169	0.822	1.687	2.203	1.151
35	337.3	0.457	0.230	0.174	0.817	1.630	2.275	1.134
36	322.5	0.451	0.213	0.181	0.808	1.646	2.325	1.178
37	309.0	0.456	0.204	0.188	0.800	1.621	2.304	1.221
38	302.5	0.449	0.195	0.183	0.804	1.569	2.366	1.244
39	280.6	0.443	0.186	0.197	0.789	1.597	2.267	1.194
40	263.5	0.448	0.175	0.210	0.775	1.578	2.221	1.231
41	246.6	0.438	0.163	0.213	0.771	1.538	2.221	1.177
42	235.5	0.433	0.155	0.223	0.758	1.561	2.195	1.220
43	216.0	0.431	0.144	0.238	0.741	1.539	2.116	1.228
44	196.0	0.428	0.122	0.263	0.712	1.555	2.181	1.290
45	176.0	0.429	0.096	0.277	0.695	1.475	2.428	1.195
46	216.0	0.420	0.144	0.242	0.736	1.607	2.102	1.233
47	270.9	0.394	0.192	0.202	0.781	1.781	2.103	1.208
48	291.5	0.365	0.230	0.177	0.810	1.806	1.953	1.094
49	325.5	0.342	0.280	0.158	0.828	1.907	1.831	1.348
50	365.5	0.312	0.338	0.151	0.838	2.232	1.716	1.272
51	393.5	0.293	0.386	0.130	0.862	2.200	1.663	1.132
52	428.5	0.245	0.473	0.125	0.869	2.753	1.488	1.050
53	464.8	0.216	0.552	0.124	0.872	3.322	1.386	1.027
54	484.4	0.186	0.626	0.122	0.873	3.985	1.276	1.161
55	498.0	0.151	0.675	0.119	0.876	4.907	1.220	1.288
56	510.0	0.136	0.719	0.117	0.880	5.443	1.177	1.185
57	518.5	0.115	0.747	0.114	0.883	6.382	1.155	1.274
58	523.0	0.103	0.786	0.114	0.883	7.141	1.109	1.386
59	531.0	0.089	0.814	0.116	0.882	8.572	1.085	1.465
60	542.0	0.058	0.878	0.106	0.891	12.22	1.037	2.348
				Run 11				
1	224.7	0.092	0.292	0.104	0.870	3.242	1.277	1.108
2	227.0	0.156	0.275	0.152	0.826	2.851	1.301	1.000
3	242.0	0.247	0.235	0.179	0.800	2.251	1.567	1.141
4	244.3	0.330	0.201	0.192	0.788	1.827	1.822	1.165
5	247.0	0.471	0.157	0.219	0.765	1.472	2.291	1.263
6	243.5	0.593	0.120	0.236	0.749	1.244	2.886	1.502
7	228.0	0.699	0.084	0.271	0.715	1.135	3.693	1.757
8	200.5	0.781	0.054	0.325	0.661	1.079	4.685	1.927
9	176.0	0.860	0.032	0.404	0.584	1.071	6.039	2.305

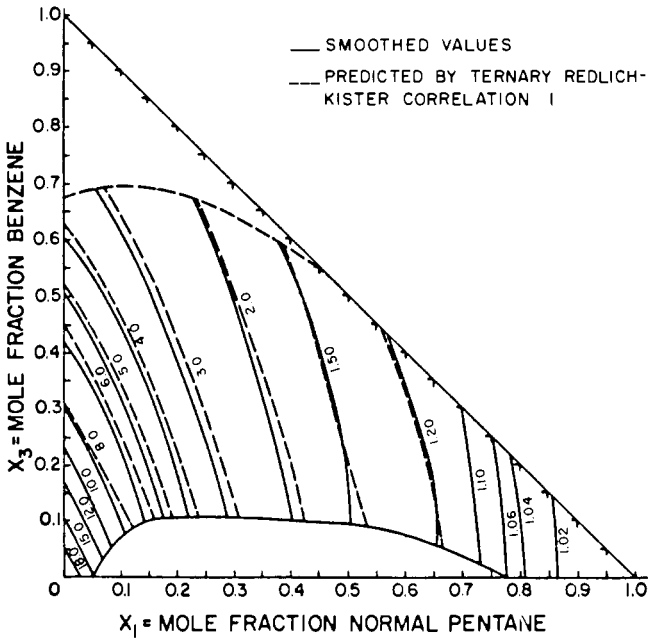

Figure 5. *n*-Pentane constant activity coefficient curves

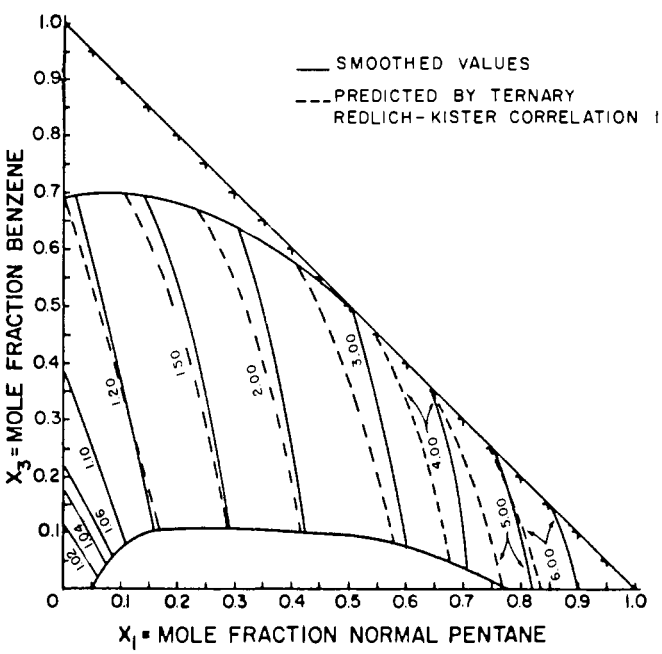

Figure 6. Sulfur dioxide constant activity coefficient curves

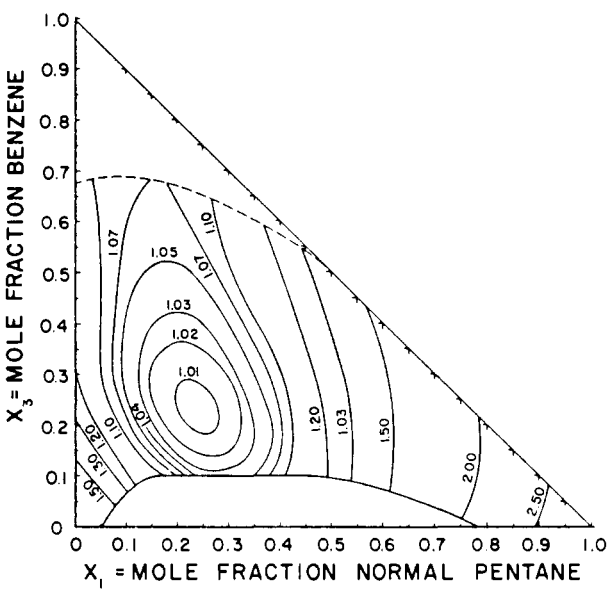

Figure 7. Smoothed values of benzene constant activity coefficient curves

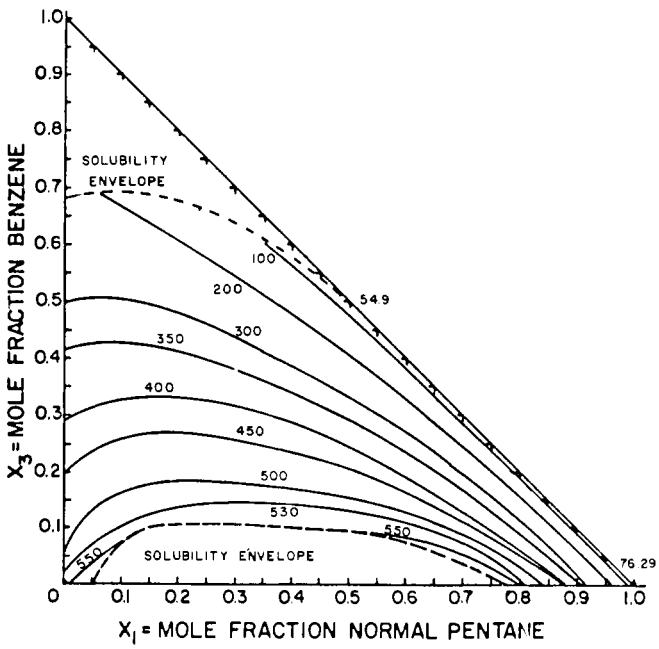

Figure 8. Isobars of total pressure (mm. of Hg) calculated from smoothed activity coefficients

which are based on use of the dimensionless excess free energy, $Q = \sum x_i \log \gamma_i$. For a ternary system Q is approximated by Equation 9.

$$Q_{123} = \sum_{i=1}^{2} \sum_{j>i}^{3} \{x_i x_j[B_{ij} + C_{ij}(x_i - x_j) + D_{ij}(x_i - x_j)^2 + \ldots]\} + x_1 x_2 x_3[C + D_1(x2 - x_3) + D_2(x_1 x_3) + \ldots] \quad (9)$$

where B_{ij}, C_{ij}, and D_{ij} are binary constants and C, D_1, D_2, ... are ternary constants. Smith (*15*) has shown that expressions for log γ_r derived from Equation 9 can be expressed in general form, which for present purposes are written as

$$\log \gamma_r = F_r(B_{ij}, C_{ij}, D_{ij}, C, D_1, D_2, X_i, X_j) \quad (10)$$

The dashed curves in Figures 5 and 6 and the curves in Figure 9 were obtained by fitting the ternary data by least squares to the expression:

$$\log \frac{\gamma_{i,\text{exp.}}}{\gamma_{i,\text{Bin.}}} = C f_{C,i}(x_i, x_j) + D_1 f_{D_1,i}(x_i, x_j) + D_2 f_{D_2,i}(x_i, x_j) \quad (11)$$

where $\gamma_{i,\text{Bin.}} = \gamma_i$ calculated from Equation 10 using only the binary constants given in Table III; and $f_{C,i}$, $f_{D_1,i}$, $f_{D_2,i}$ = coefficients of the ternary constants in the ternary Redlich-Kister expression for log γ_i. The least squares fit was carried out by the procedure discussed in connection with Equations 6, 7, and 8 (Ternary Correlation I). Values of constants C, D_1, and D_2 obtained are given in Table VI. Inspection of Figure 9 shows that in the vicinity of $x_1 = 0.25$, $x_3 = 0.20$, γ_3 was predicted to be less than unity. Since this was contrary to what one would expect from physical considerations, the consistency of activity coefficients in this region was carefully checked. A form of the Gibbs-Duhem equation was integrated numerically using predicted activity coefficients to six decimal places at several values of x_2.

Table V. Benzene Activity Coefficients in *n*-Pentane (1)–Sulfur Dioxide (2)–Benzene (3) System in Presence of Solid Benzene

Sample	x_1	x_2	x_3	$\gamma_{3\,exp.}$[a]	$\gamma_{3\,pred.}$[b]	$\Delta\gamma_3$
1	0.4663	...	0.5337	1.355	1.30685	0.04815
2	...	0.3202	0.6798	1.065	1.00531	0.05969
3	0.0280	0.2829	0.6891	1.050	0.99480	0.05520
4	0.0453	0.2699	0.6848	1.056	0.99480	0.06435
5	0.0636	0.2458	0.6906	1.048	0.99165	0.05825
6	0.0937	0.2142	0.6921	1.046	0.98975	0.05499
7	0.1146	0.1999	0.6855	1.056	0.99101	0.06187
8	0.1397	0.1761	0.6842	1.058	0.99413	0.05708
9	0.1644	0.1582	0.6773	1.068	1.00975	0.05825
10	0.4170	0.0194	0.5636	1.284	1.23284	0.05116

[a] $\gamma_3 = (0.7237)/(x_3)$ (Equation 5). [b] Predicted by Ternary Correlation II.

Table VI. Summary of Redlich-Kister Constants for Correlation of Ternary Data[a]

Correlation	Constant	Value
I	C	−0.2270
	D_1	−0.3682
	D_2	0.7698
II	B_{12}	1.1511
	C_{12}	−0.2637
	B_{13}	0.5462
	C_{13}	0.1050
	B_{23}	0.2499
	C_{23}	0.2583
	C	−0.3451
	D_1	−1.0645
III	B_{12}	1.1155
	C_{12}	−0.2307
	B_{13}	0.5379
	C_{13}	0.0029
	B_{23}	0.2396
	B_{23}	0.1262
	C	−0.2192
	D_1	−0.1280

[a] See Table III for values of binary constants obtained from binary data.

In three integrations across Figure 9 at $x_2 = 0.60$, 0.55, and 0.50, discrepancies of 7×10^{-8}, 1.7×10^{-7}, and 1.4×10^{-7} were obtained. These results are an independent check on the computer program used in the Redlich-Kister correlation. Furthermore, inspection of the various terms of the Redlich-Kister equation makes it clear that values of γ_3 less than 1 can be predicted in this region.

In another correlation (Ternary Correlation II), binary and ternary data were fitted simultaneously using six binary and two ternary constants in Equation 10. In Ternary Correlation II the binary data were treated in the same fashion as the ternary, except that the activity coefficient of the absent component was given a fictitious value and a weight of zero. In Ternary Correlation III the ternary data alone were fitted to the expression used in Correlation II.

These three correlations were compared by considering the values of S_m for each component, the total S_m for all components, and the Gauss criterion, Ω, defined by Equation 12

$$\Omega = \frac{S_m}{N_t - N_c} \tag{12}$$

Values of S_m and Ω for the three correlations are given in Table VIII (deposited with ADI). Correlation II gave lower values for S_m for sulfur dioxide and benzene and a higher value for *n*-pentane than I. Correlation III gave lower values of S_m, for all components than Correlation I. This is to be expected, since no binary constants determined previously from binary data are being imposed upon the ternary results. Correlation III gave lower values of S_m than Correlation II for all components except sulfur dioxide.

Table VII. Phase Equilibrium and Activity Coefficient Data for the Quaternary System *n*-Pentane(1)–Sulfur Dioxide(2)–Benzene(3)–*n*Hexane(4) at 0° F.

Sample	Pressure	Component	x_i	y_i	γ_i
1	547.0	1	0.016	0.023	9.643
		2	0.984	0.977	1.023
2	557.5	1	0.023	0.064	19.264
		2	0.977	0.936	1.006
3S	570.5	1	0.030	0.068	16.152
		2	0.954	0.914	1.028
		4	0.016	0.017	35.170
4S	547.5	1	0.035	0.071	13.591
		2	0.911	0.915	1.036
		3	0.033	0.001	1.413
		4	0.021	0.013	19.315
5S	534.0	1	0.044	0.075	11.266
		2	0.868	0.910	1.055
		3	0.059	0.001	1.361
		4	0.029	0.013	13.802
6S	525.0	1	0.051	0.069	8.914
		2	0.836	0.911	1.079
		3	0.075	0.002	1.368
		4	0.038	0.017	12.994
7S	515.0	1	0.057	0.067	7.562
		2	0.795	0.915	1.117
		3	0.093	0.002	1.409
		4	0.055	0.015	8.314
8S	522.0	1	0.048	0.062	8.308
		2	0.816	0.920	1.110
		3	0.087	0.002	1.381
		4	0.048	0.015	9.309
9S	516.0	1	0.042	0.057	8.716
		2	0.827	0.923	1.086
		3	0.083	0.002	1.482
		4	0.048	0.018	10.946
10S	515.0	1	0.035	0.012	2.178
		2	0.832	0.965	1.126
		3	0.081	0.002	1.468
		4	0.052	0.021	11.510
11S	507.0	1	0.047	0.050	6.779
		2	0.781	0.926	1.134
		3	0.103	0.002	1.335
		4	0.069	0.021	8.767
12S	498.5	1	0.050	0.047	5.853
		2	0.754	0.928	1.158
		3	0.110	0.003	1.354
		4	0.086	0.022	7.149
13S	489.6	1	0.133	0.049	2.250
		2	0.483	0.925	1.768
		3	0.132	0.003	1.247
		4	0.251	0.023	2.542
14S	475.0	1	0.126	0.046	2.167
		2	0.468	0.926	1.776
		3	0.147	0.003	1.264
		4	0.259	0.024	2.536
15	458.0	1	0.132	0.043	1.880
		2	0.419	0.929	1.921
		3	0.176	0.004	1.247
		4	0.273	0.023	2.167
16	441.5	1	0.124	0.040	1.793
		2	0.396	0.931	1.964
		3	0.204	0.005	1.139
		4	0.276	0.024	2.155
3R	570.5	1	0.432	0.068	1.115
		2	0.176	0.913	5.574
		4	0.392	0.018	2.901
4R	547.5	1	0.418	0.071	1.145
		2	0.229	0.915	4.123
		3	0.034	0.001	1.377
		4	0.319	0.013	1.256
5R	534.0	1	0.391	0.075	1.269
		2	0.277	0.910	3.311
		3	0.061	0.001	1.318
		4	0.271	0.013	1.471
6R	525.0	1	0.358	0.069	1.268
		2	0.293	0.912	3.081
		3	0.076	0.002	1.341
		4	0.272	0.017	1.815
7R	515.5	1	0.315	0.067	1.363
		2	0.324	0.915	2.714
		3	0.092	0.002	1.429
		4	0.268	0.016	1.701
8R	522.0	1	0.314	0.062	1.283
		2	0.303	0.920	2.993
		3	0.083	0.002	1.456
		4	0.300	0.015	1.486

(*Continued on page 303*)

Table VII. Phase Equilibrium and Activity Coefficient Data for the Quaternary System *n*-Pentane(1)–Sulfur Dioxide(2)–Benzene(3)–*n*-Hexane(4) at 0° F. (*Continued*)

Sample	Pressure	Component	x_i	y_i	γ_i
9R	516.5	1	0.281	0.057	1.292
		2	0.305	0.923	2.949
		3	0.086	0.002	1.437
		4	0.328	0.018	1.621
10R	515.0	1	0.235	0.012	0.320
		2	0.310	0.965	3.024
		3	0.087	0.002	1.353
		4	0.367	0.021	1.645
11R	507.0	1	0.212	0.050	1.492
		2	0.337	0.926	2.625
		3	0.098	0.002	1.403
		4	0.353	0.021	1.708
12R	498.5	1	0.180	0.047	1.630
		2	0.387	0.928	2.254
		3	0.114	0.003	1.305
		4	0.318	0.022	1.928
13R	489.6	1	0.137	0.049	2.175
		2	0.483	0.925	1.769
		3	0.139	0.003	1.183
		4	0.240	0.023	2.662
14R	475.0	1	0.133	0.046	2.055
		2	0.461	0.926	1.803
		3	0.154	0.004	1.206
		4	0.252	0.024	2.607
15	458.0	1	0.121	0.043	2.052
		2	0.422	0.929	1.909
		3	0.178	0.004	1.233
		4	0.279	0.023	2.118

Quaternary Data. The experimental data on the *n*-pentane–sulfur dioxide–benzene–*n*-hexane system are given in Table VII. The sample numbers in Table VII followed by an S or an R indicate that the system consisted of two liquids and a vapor phase. The data were correlated by the least squares procedure described above, using eight binary Redlich-Kister constants, and results are given in Table IX (deposited with ADI). The fit was generally not adequate. The Redlich-Kister constants obtained were:

$B_{12} = 2.2293$, $C_{12} = 1.3477$, $B_{13} = -0.5826$, $B_{23} = 0.1757$, $B_{14} = -0.6949$, $B_{24} = 1.316$, $C_{23} = -0.1612$, $B_{34} = 1.657$.

No further correlation work on the quaternary data was done because it was believed that the usual integrated forms (Redlich-Kister, Margules, Van Laar, etc.) would not be adequate for such systems. The quaternary data were obtained for use in the development of more powerful correlation methods and are reported here because of the scarcity of such data. No consistency checks were made, but the quality of the ternary data taken earlier furnished some indirect evidence concerning the accuracy of the four-component activity coefficient measurements.

ACKNOWLEDGMENT

The authors are indebted to the Humble Oil and Refining Co. for financial support. W. W. Bowden is indebted to the Board of Managers of Rose Polytechnic Institute for a leave of absence and for financial support.

NOMENCLATURE

$\bar{a}_B$ = activity of benzene in solution
a_B^s = activity of benzene as a solid
B_i = second virial coefficient of component i, cu. ft./lb. mole
B_{ij} = binary Redlich-Kister constant
C_{ij} = binary Redlich-Kister constant
D_{ij} = binary Redlich-Kister constant
C, D_1, D_2 = ternary Redlich-Kister constants
f_B° = fugacity of benzene in its standard state
$\bar{f}_B$ = fugacity of benzene in solution
$f_{B,p}^L$ = fugacity of benzene as a liquid at total pressure of system
$f_i[B_{ij}, D_{ij}, X_i(k)]$ = function defined by some Redlich-Kister expression, typically an expression such as right-hand side of Equation 6
F_r = function defined by Equation 2-53 in (*15*)
N_c = number of constants in Redlich-Kister expression
N_k = number of data points
Q = $\sum x_i \log \gamma_i$
$R_{i,k}$ = residual function for ith component, and kth data point, defined by equation 7
R = universal gas constant, (atm.)(cc.)/(deg.)(mole)
S_m = sum of squares of deviations of experimental activity coefficients from those predicted by some correlation
T = absolute temperature
$f_{C,i}$ = coefficient of ternary constant C in Redlich-Kister expression for $\log \gamma_i$
$f_{D,i}$ = coefficient of ternary constant D_i in Redlich-Kister expression for $\log \gamma_i$
n = number of data points in set of data
p = total pressure of system
p_i^* = vapor pressure of pure i
x_i = mole fraction of i in liquid solution
y_i = mole fraction of i in gaseous solution
γ_i = activity coefficient of component i. Subscript B refers to benzene in Equations 3 to 5
$\gamma_{i,\text{Bin.}}$ = value of γ_i calculated by Redlich-Kister expression using constants obtained from binary data
$\gamma_{i,\text{exp.}}$ = experimental value of γ_i, calculated from Equation 1
Ω = Gauss criterion, defined by Equation 12

LITERATURE CITED

(1) Bottomley, G.A., Reeves, C.G., *Trans. Faraday Soc.* **53**, 1455 (1957).
(2) Bowden, W.W., Ph.D. thesis, Purdue University, West Lafayette, Ind., 1965.
(3) Dodge, B.F., "Chemical Engineering Thermodynamics," p. 562, McGraw-Hill, New York, 1944.
(4) Maxwell, J.B., "Data Book on Hydrocarbons," Van Nostrand, New York, 1950.
(5) Myers, H.S., *Ind. Eng. Chem.* **47**, 2215-19 (1955).
(6) Pitzer, K.S., Curl, R.F., Jr., *J. Am. Chem. Soc.* **79**, 2369 (1957).
(7) Redlich, O., Kister, A.T., *Ind. Eng. Chem.* **40**, 341-5 (1948).
(8) Rossini, F.D., "Selected Values of Physical and Thermodynamic Properties of Hydrocarbons and Related Compounds," API Project 44, p. 336, Carnegie Press, Pittsburgh, 1953.
(9) Rynning, D.F., Hurd, C.O., *Trans. A.I.Ch.E.* **41**, 265 (1945).
(10) Satterfield, C.N., Powell, J.H., Jr., Oster, E.A., Jr., Noyes, J.P., *Ind. Eng. Chem.* **47**, 1458 (1955).
(11) Schuhmann, R., Jr., *Acta Met.* **3**, 219-26 (1955).
(12) Smirnova, N.A., Morachevsky, A.V., Storonkin, A.V., *Vestn. Leningrad Univ.*, No. **22**, 97-104 (1963).
(13) Smith, B.D., "Design of Equilibrium Stage Processes," pp. 40-2, McGraw-Hill, New York, 1963.
(14) *Ibid.*, p. 53.
(15) *Ibid.*, p. 58.
(16) Smith, B.D., Bowden, W.W., *Anal. Chem.* **36**, 82 (1964).
(17) *Ibid.*, p. 87.
(18) Udovenko, V.V., Fatkulina, L.G., *Zhur. Fiz. Khim.* **26**, 1438-47 (1952).

RECEIVED for review June 21, 1965. Accepted April 11, 1966. Material supplementary to this article has been deposited as Document No. 8889 with the ADI Auxiliary Publications Project, Photoduplication Service, Library of Congress, Washington 25, D. C. A copy may be secured by citing the document number and by remitting $1.25 for photoprints or $1.25 for 35-mm. microfilm. Advance payment is required. Make checks or money orders payable to Chief, Photoduplication Service, Library of Congress.